Residues in the Seventh Membrane-Spanning Segment of the Dopamine D2 Receptor Accessible in the Binding-Site Crevice†

Dingyi Fu,‡ Juan A. Ballesteros,§ Harel Weinstein,§ Jiayun Chen,‡ and Jonathan A. Javitch*,‡,||

Center for Molecular Recognition and Department of Psychiatry and Pharmacology, College of Physicians and Surgeons, Columbia University, 630 West 168th Street, New York, New York 10032, and Department of Physiology and Biophysics, Mount Sinai School of Medicine, New York, New York 10029

Received April 16, 1996; Revised Manuscript Received June 3, 1996⊗

ABSTRACT: The binding site of the dopamine D2 receptor, like that of other homologous G-protein-coupled receptors, is contained within a water-accessible crevice formed among its seven membrane-spanning segments. Using the substituted-cysteine accessibility method, we previously mapped the residues that form the surface of the binding-site crevice in the third and fifth membrane-spanning segments (M3 and M5). We have now mutated to cysteine, one at a time, 26 consecutive residues in and flanking the seventh membrane-spanning segment (M7) and expressed the mutant receptors in HEK 293 cells. Nine of these mutants reacted with charged, hydrophilic, lipophobic, sulfhydryl-specific reagents, added extracellularly, and were protected from reaction by a reversible dopamine antagonist, sulpiride. Thus, we infer that the side chains of these residues are in the water-accessible surface of the binding-site crevice. The pattern of accessibility of the cysteine-substitution mutants is consistent with M7 being a kinked α-helix.

The dopamine receptors, like the homologous receptors for the other biogenic amines, bind neurotransmitters present in the extracellular medium and couple this binding to the activation of intracellular G-proteins (Civelli et al., 1991; Strader et al., 1994). The binding sites of these receptors are formed among their seven, mostly hydrophobic, membrane-spanning segments (Oprian, 1992; Strader et al., 1994) and are accessible to charged, water-soluble agonists, like dopamine. Thus, for each of these receptors, the binding site is contained within a water-accessible crevice, the binding-site crevice, extending from the extracellular surface of the receptor into the plane of the membrane. The surface of this crevice is formed by residues that can contact specific agonists and/or antagonists and by other residues that may play a structural role and affect binding indirectly.

To identify the residues that form the surface of the binding-site crevice in the human D2 receptor, we have used the substituted-cysteine accessibility method (SCAM)[1] (Akabas et al., 1992, 1994; Javitch et al., 1994, 1995a,b). Consecutive residues in the membrane-spanning segments are mutated to cysteine, one at a time, and the mutant receptors are expressed in heterologous cells. If ligand binding to a cysteine-substitution mutant is near-normal, we assume that the structure of the mutant receptor, especially around the binding site, is similar to that of wild type and that the substituted cysteine lies in an orientation similar to that of the wild-type residue. In the membrane-spanning segments, the sulfhydryl of a cysteine can face either into the binding-site crevice, into the interior of the protein, or into the lipid bilayer; sulfhydryls facing into the binding-site crevice should react much faster with hydrophilic, lipophobic, sulfhydryl-specific reagents. For such reagents, we use derivatives of methanethiosulfonate (MTS): positively charged MTSethylammonium (MTSEA) and MTSethyltrimethylammonium (MTSET) and negatively charged MTSethylsulfonate (MTSES) (Stauffer & Karlin, 1994). These reagents are about the same size as dopamine, with maximum dimensions of approximately 10 Å by 6 Å. They form mixed disulfides with the cysteine sulfhydryl, covalently linking SCH_2CH_2X, where X is NH_3^+, $N(CH_3)_3^+$, or SO_3^-. We use two criteria for identifying an engineered cysteine as forming the surface of the binding-site crevice: (i) the reaction with a MTS reagent alters binding irreversibly and (ii) this reaction is retarded by the presence of agonists or antagonists. The binding regions for agonists and antagonists in the D2 and related receptors may be similar but not identical (Barak et al., 1995; Javitch et al., 1996; Kozell et al., 1994; MacKenzie et al., 1993). We have used sulpiride because antagonists are less likely to cause conformational changes which may complicate the interpretation of the protection experiment in which the reaction with a MTS reagent is retarded in the presence of a specific receptor ligand.

We previously found that antagonist binding to wild-type D2 receptor was irreversibly inhibited by MTSEA and MTSET and that Cys118, in the third membrane-spanning segment (M3), was responsible for this sensitivity (Javitch et al., 1994). Therefore, we used the mutant C118S, which is insensitive to MTS reagents, as the background for further mutation. In our initial application of SCAM to the D2

† This work was supported in part by NIMH Grants MH01030 and MH54137, by NIH Training Grant NS07258, by the G. Harold & Leila Y. Mathers Charitable Trust (J.A.J.), and by NIDA Grants DA09083 and DA00060 (H.W.).

‡ Center for Molecular Recognition, Columbia University.

§ Mount Sinai School of Medicine.

|| Department of Psychiatry and Pharmacology, Columbia University.

⊗ Abstract published in *Advance ACS Abstracts,* August 1, 1996.

[1] Abbreviations: SCAM, substituted-cysteine accessibility method; M3, the third membrane-spanning segment; M5, the fifth membrane-spanning segment; M7, the seventh membrane-spanning segment; MTS, methanethiosulfonate; MTSEA, MTSethylammonium; MTSET, MTSethyltrimethylammonium; MTSES, MTSethylsulfonate; GPCRs, G-protein-coupled receptors; Pro kink, proline kink.

S0006-2960(96)00928-2 CCC: $12.00

receptor (Javitch et al., 1995a), we found that 10 of 23 residues tested in the M3 segment are in the water-accessible surface of the binding-site crevice. From the pattern of accessibility, we inferred that M3 forms an α-helix, one side of which faces the binding-site crevice. Additionally, we found that 13 of 24 residues tested in the fifth membrane-spanning segment (M5) are in the water-accessible surface of the binding-site crevice (Javitch et al., 1995b). Of the 13 accessible residues, 10 were consecutive. This pattern is inconsistent with M5 being a fixed α-helix, one side of which is accessible in the binding-site crevice.

On the basis of site-directed mutagenesis experiments, many laboratories have implicated residues in the seventh membrane-spanning segment (M7) of G-protein-coupled receptors (GPCRs) in binding and in receptor activation (van Rhee & Jacobson, 1996). In addition, a Trp in M7 of the β-adrenergic receptor was photolabeled by an antagonist derivative (Wong et al., 1988). This residue is highly conserved in other biogenic amine receptors, including the D2 receptor. In this paper, we report the application of SCAM to identify systematically all the residues in M7 of the D2 receptor that contribute to the binding-site crevice.

EXPERIMENTAL PROCEDURES

Numbering of Residues. The positions of all residues in the human $D2_L$ receptor sequence are given. In some cases, we also index residues relative to the most conserved residue in the membrane-spanning segment in which it is located (Ballesteros & Weinstein, 1995). By definition, the most conserved residue is assigned the position index 50, e.g. Pro423$^{(7.50)}$, and therefore Asn422$^{(7.49)}$ and Ile424$^{(7.51)}$. This indexing simplifies the identification of corresponding residues in comparisons and sequence alignments of different GPCRs.

Site-Directed Mutagenesis. Cysteine mutations were generated as described previously (Javitch et al., 1995a). Mutations were confirmed by DNA sequencing. Mutants are named as (wild-type residue)(residue number)(mutant residue), where the residues are given in the single-letter code.

Transient Transfection. HEK 293 cells were grown in DMEM/F12 (1:1) containing 3.15 g/L glucose in 10% bovine calf serum at 37 °C and 5% CO_2. Thirty-five millimeter dishes of 293 cells at 60−80% confluence were cotransfected with 1 μg of wild-type or mutant D2 receptor cDNA in pcDNAI/Amp (Invitrogen) and 0.2 μg of pRSVTag using 9 μL of lipofectamine (Gibco) and 1 mL of OPTIMEM (Gibco). Five hours after transfection, the plates were diluted with 1 mL of media containing 20% bovine calf serum. Twenty-four hours after transfection, the medium was changed. Forty-eight hours after transfection, cells were washed with phosphate-buffered saline [PBS; 8.1 mM NaH_2PO_4, 1.5 mM KH_2PO_4, 138 mM NaCl, and 2.7 mM KCl (pH 7.2)], briefly treated with PBS containing 5 mM EDTA, and then dissociated in PBS. Cells were pelleted at 1000*g* for 5 min at 4 °C and resuspended for binding or treatment with MTS reagents.

[^{3}H]-N-Methylspiperone Binding. Whole cells were suspended in 450 μL of buffer A [25 mM HEPES, 140 mM NaCl, 5.4 mM KCl, 1 mM EDTA, and 0.006% BSA (pH 7.4)]. Cells were then diluted 20-fold with buffer A. [^{3}H]-*N*-Methylspiperone (Dupont/NEN) binding was performed as described previously (Javitch et al., 1995b). For saturation binding, duplicate borosilicate tubes contained six different concentrations of [^{3}H]-*N*-methylspiperone between 5 and 800 pM in buffer A with 300 μL of cell suspension in a final volume of 0.5 mL. The mixture was incubated at room temperature for 60 min and then filtered using a Brandel cell harvester through Whatman 934AH glass fiber filters (Brandel). The filter was washed twice with 5 mL of 10 mM Tris-HCl and 120 mM NaCl (pH 7.4) at room temperature. Specific [^{3}H]-*N*-methylspiperone binding was defined as total binding less nonspecific binding in the presence of 1 μM (+)-butaclamol (Research Biochemicals).

Reactions with MTS Reagents. Whole cells were suspended in 450 μL buffer A. Aliquots (50 μL) of cell suspension were incubated with freshly prepared MTS reagents at the stated concentrations at room temperature for 2 min. Cell suspensions were then diluted 20-fold, and 300 μL aliquots were used to assay for [^{3}H]-*N*-methylspiperone (300 pM) binding as described above. The fractional inhibition was calculated as 1 − (specific binding after MTS reagent)/(specific binding without reagent). We used the SPSS for Windows (SPSS, Inc.) statistical software to analyze the effects of the MTS reagents by one-way ANOVA according to Duncan's post hoc test ($p < 0.05$).

The second-order rate constant (k) for the reaction of MTSEA with each susceptible mutant was estimated by determining the extent of reaction after a fixed time, 2 min, with four concentrations of MTSEA (0.1, 0. 25, 1, and 2.5 mM) (all in excess over the reactive sulfhydryls). The fraction of initial binding, Y, was fit to e^{-kct}, where k is the second-order rate constant, c is the concentration of MTSEA, and t is the time (120 s).

RESULTS

Effects of Cysteine Substitution on Antagonist Binding. In a background of the mutant C118S, we mutated to cysteine, one at a time, 26 consecutive residues, Val406 to Ile431, from the extracellular loop between M6 and M7 to near the end of M7. Each mutant receptor was transiently expressed in HEK 293 cells, and the K_D and B_{MAX} characterizing the equilibrium binding of the radiolabeled antagonist, [^{3}H]-*N*-methylspiperone, were determined. At 24 positions, the K_D of the cysteine-substitution mutant was between 0.4 and 1.6 times the K_D of C118S; in Y416C, the K_D was 3 times the K_D of C118S (Table 1). For these 25 mutants, B_{MAX} ranged from 5 to 120% of that obtained with C118S (Table 1). Only the mutant G415C failed to bind [^{3}H]-*N*-methylspiperone.

The K_I of the antagonist sulpiride was determined in the 25 mutants which bound [^{3}H]-*N*-methylspiperone (Table 2). At 19 positions, the K_I was between 0.5 and 1.5 times the K_I of C118S; in the mutants N422C, P423C, and Y426C, the K_I was 2.3−3.3 times the K_I of C118S. In Y416C, N418C, and S419C, the K_I was 185, 5, and 8 times the K_I of C118S, respectively.[2]

Reactions of the Mutants with MTSEA. We tested the effects of 2.5 and 0.25 mM MTSEA on the mutants. The

[2] The much greater effect of mutation of Tyr416 to Cys on sulpiride binding than on *N*-methylspiperone binding is consistent with the hypothesis that Tyr416 forms part of an accessory binding site for the substituted benzamides and piquindone, but not other antagonists (Teeter & DuRand, 1996). However, the modification of Tyr416 to a lysine-like side chain by the reaction of Y416C with MTSEA dramatically interferes with the binding of *N*-methylspiperone as well as sulpiride.

Table 1: Characteristics of [^{3}H]-*N*-Methylspiperone Binding to Cysteine-Substituted Dopamine D2 Receptor[a]

mutant	K_D (pM)	K_{MUT}/K_{C118S}	B_{MAX} (fmol/cm^2)	*n*
C118S	89 ± 5	1.0	197 ± 8	4
V406C	88 ± 26	1.0	105 ± 61	2
L407C	58 ± 14	0.7	73 ± 11	2
Y408C	130 ± 19	1.5	136 ± 21	2
S409C	88 ± 5	1.0	89 ± 28	2
A410C	88 ± 13	1.0	169 ± 45	2
F411C	75 ± 14	0.8	92 ± 30	2
T412C	74 ± 9	0.8	161 ± 23	2
W413C	143 ± 7	1.6	58 ± 24	2
L414C	71 ± 1	0.8	57 ± 14	2
G415C	no significant binding			
Y416C	266 ± 35	3.0	49 ± 2	3
V417C	75 ± 5	0.8	164 ± 38	2
N418C	66 ± 23	0.7	102 ± 11	2
S419C	53 ± 9	0.6	205 ± 8	2
A420C	63 ± 5	0.7	105 ± 6	2
V421C	106 ± 37	1.2	167 ± 19	2
N422C	35 ± 6	0.4	26 ± 1	2
P423C	45 ± 15	0.5	10 ± 6	2
I424C	45 ± 10	0.5	55 ± 21	2
I425C	69 ± 11	0.8	27 ± 7	2
Y426C	81 ± 14	0.9	39 ± 6	3
T427C	70 ± 11	0.8	242 ± 117	2
T428C	62 ± 12	0.7	260 ± 104	2
F429C	61 ± 3	0.7	189 ± 46	2
N430C	80 ± 34	0.9	183 ± 84	2
I431C	39 ± 8	0.4	34 ± 10	3

[a] Cells transiently transfected with the appropriate receptor were assayed as described in Experimental Procedures. Data were fit to the binding isotherm by nonlinear regression. The means and SEM are shown for *n* independent experiments, each with duplicate determinations. B_{MAX} values are presented as femtomoles per square centimeter of plate area.

Table 2: Inhibitory Potency of (−)-Sulpiride on [^{3}H]-*N*-Methylspiperone Binding to Cysteine-Substituted Dopamine D2 Receptor[a]

mutant	apparent K_I (nM)	*n*	$K_{I(MUT)}/K_{I(C118S)}$
C118S	8 ± 1	5	1.0
V406C	7 ± 0.4	2	0.9
L407C	11 ± 1	2	1.4
Y408C	12 ± 3	2	1.5
S409C	5 ± 2	2	0.6
A410C	7 ± 0.9	2	0.8
F411C	11 ± 0.2	2	1.4
T412C	6 ± 0.2	2	0.8
W413C	5 ± 0.7	2	0.6
L414C	8 ± 0.6	2	1.0
Y416C	1500 ± 600	2	185
V417C	13 ± 4	2	1.6
N418C	42 ± 3	2	5.2
S419C	64 ± 11	2	8.0
A420C	4 ± 0.3	2	0.5
V421C	6 ± 1	2	0.8
N422C	24 ± 0.3	2	3.1
P423C	27 ± 5	2	3.3
I424C	4 ± 0.1	2	0.5
I425C	5 ± 1	2	0.7
Y426C	18 ± 0.3	2	2.3
T427C	8 ± 0.7	2	1.0
T428C	5 ± 0.2	2	0.6
F429C	5 ± 0.2	2	0.7
N430C	5 ± 0.2	2	0.6
I431C	4 ± 0.0	2	0.5

[a] Cells transiently transfected with the appropriate receptor were assayed with [^{3}H]-*N*-methylspiperone (80 pM) as described in Experimental Procedures in the presence of nine concentrations of (−)-sulpiride. The apparent K_I was determined by the method of Goldstein and Barrett (1987) using the IC_{50} value obtained by fitting the data to a one-site competition model by nonlinear regression. The means and SEM are shown for *n* independent experiments, each with duplicate determinations.

higher concentration significantly blocked [^{3}H]-*N*-methylspiperone binding at 12 of 25 positions (Figure 1A). The lower concentration significantly blocked binding to seven of these mutants (Figure 1B). To quantitate the susceptibility to MTSEA, we determined the second-order rate constants for the reaction with MTSEA (Table 3). The most reactive cysteines were those substituted for Trp413 and Tyr416. Cysteines substituted for Leu407, Phe411, and Thr412 were of intermediate reactivity with MTSEA. Cysteines substituted for Ser409, Asn418, Asn422, Pro423, and Tyr426 were less reactive, and Tyr408 and Ala410 were least reactive. The reversible antagonist sulpiride significantly retarded the reaction of MTSEA with L407C, F411C, T412C, W413C, Y416C, N418C, N422C, P423C, and Y426C.[3] The degree of protection varied from 15 to 70% (Figure 2). In contrast, sulpiride did not slow the reaction of S409C with MTSEA.

Reactions with MTSET and MTSES. All seven of the mutants most sensitive to MTSEA (Figure 1B) were susceptible to reaction with MTSET (Figure 3A); in addition, Y426C, which was susceptible to 2.5 mM MTSEA, was also susceptible to reaction with MTSET. Although MTSEA reacted most rapidly with F411C, W413C, and Y416C, 1 mM MTSET inhibited T412C substantially more than it did these other mutants. MTSES, the negatively charged derivative, significantly inhibited binding to four of the eight mutants that were susceptible to MTSET (Figure 3B).

[3] The inhibition of T408C and A410C by 2.5 mM MTSEA was too small to test for protection reliably.

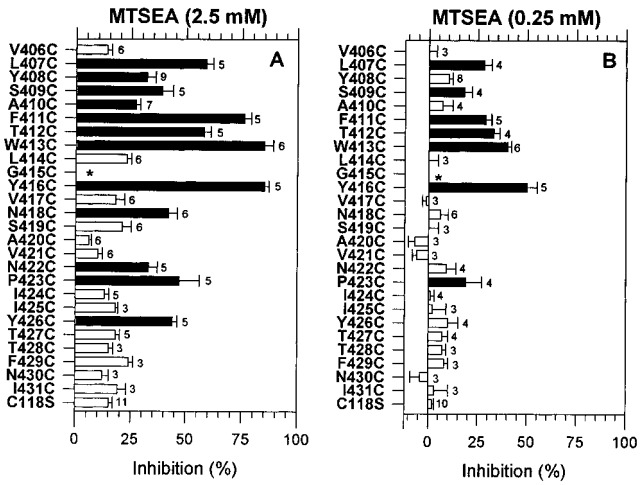

FIGURE 1: Inhibition of specific [^{3}H]-*N*-methylspiperone (300 pM) binding to intact cells transiently transfected with wild-type or mutant D2 receptors resulting from a 2 min application of (A) 2.5 mM MTSEA or (B) 0.25 mM MTSEA. The means and SEM are shown. The number of independent experiments for each mutant is shown next to the bars. Solid bars indicate mutants for which inhibition was significantly different ($p < 0.05$) than that for C118S by one-way ANOVA. * represents no detectable binding.

DISCUSSION

Residues Forming the Water-Accessible Surface of the Binding-Site Crevice. We identify residues on the water-accessible surface of the D2 receptor by the ability of the MTS reagents to react with substituted-cysteine residues. We

Table 3: Rates of Reaction of MTSEA with Cysteine-Substituted Dopamine D2 Receptor[a]

mutant	k_{MTSEA} (M^{-1} s^{-1})	k_{MUT}/k_{WT}	*n*
L407C	4.0 ± 0.3	0.10	4
Y408C	1.2 ± 0.3	0.03	6
S409C	2.3 ± 0.7	0.06	4
A410C	0.9 ± 0.2	0.02	4
F411C	6.6 ± 1.1	0.17	4
T412C	4.1 ± 0.9	0.11	3
W413C	11.5 ± 2.5	0.30	5
Y416C	11.4 ± 1.3	0.29	5
N418C	2.0 ± 0.4	0.05	5
N422C	1.6 ± 0.5	0.04	3
P423C	2.9 ± 0.5	0.07	4
Y426C	2.4 ± 0.2	0.06	2

[a] The second-order rate constant (*k*) was determined as described in Experimental Procedures. The means and SEM of *n* independent experiments, each performed with triplicate determinations, are shown. k_{MUT}/k_{WT} was obtained by dividing each *k* value by the *k* determined for the wild-type receptor in which Cys118 reacts (not C118S, which does not react and which is the background for all the other mutants).

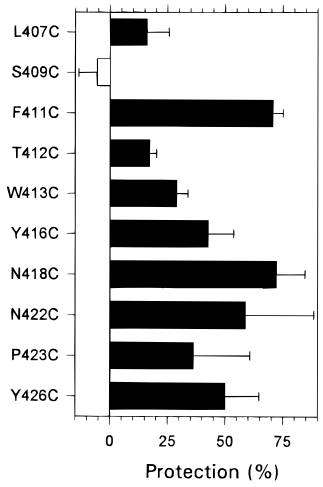

FIGURE 2: Sulpiride protection of cysteine-substitution mutants. Dissociated cells were incubated in buffer A for 20 min at room temperature in the presence or absence of (±)-sulpiride, and then MTSEA was added, in the continued presence or absence of sulpiride, for 2 min at a concentration chosen to inhibit 50−75% of specific [^{3}H]-*N*-methylspiperone binding in the absence of sulpiride. Concentrations of MTSEA were as follows: 2.5 mM for S409C, N418C, N422C, P423C, and Y426C; 1 mM for L407C, F411C, and T412C; and 0.25 mM for W413C and Y416C. For most mutants, sulpiride was used at a concentration of 10 μM. To compensate for changes in the K_I, sulpiride concentrations were adjusted for several mutants as follows: 3 μM for W413C; 50 μM for N418C, N422C, P423C, and Y426C; and 200 μM for Y416C. Cells were washed by filtration though 96-well multiscreen plates containing GFB filters (Millipore). In the wash buffer, sodium was replaced by choline in order to facilitate removal of residual sulpiride. [^{3}H]-*N*-Methylspiperone binding to the washed cells was performed in buffer A in the multiscreen plates in a final volume of 0.25 mL. The means and SEM of three to five independent experiments, each performed with triplicate determinations, are shown. Protection was calculated as 1 − (inhibition in the presence of sulpiride)/(inhibition in the absence of sulpiride). Protection by sulpiride was significant ($p < 0.05$) by paired *t* test for all of the mutants (filled bars) except S409C (unfilled bar).

assume that the MTS reagents will only react with water-accessible cysteine residues because the reagents are highly polar. Furthermore, they react 5×10^9 times faster with ionized thiolates than with un-ionized thiols (Roberts et al., 1986), and only water-accessible cysteines are likely to ionize. We infer that the MTS reagents have reacted if the

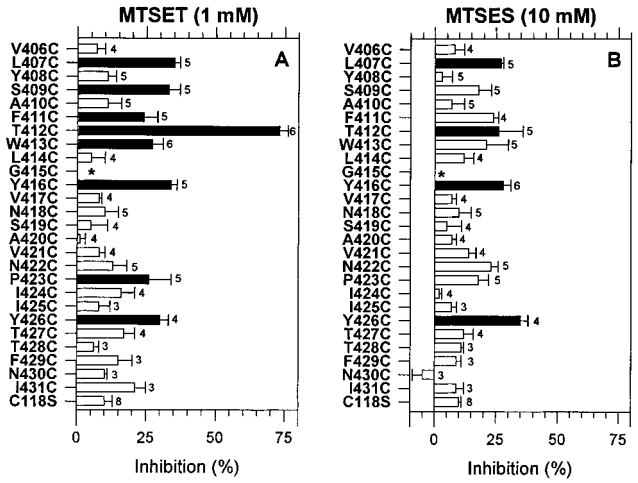

FIGURE 3: Inhibition of specific [^{3}H]-*N*-methylspiperone (300 pM) binding to intact cells transiently transfected with wild-type or mutant D2 receptors resulting from a 2 min application of (A) 1 mM MTSET or (B) 10 mM MTSES. On the basis of relative rate constants for reaction with simple thiols in solution, namely 10:4:1 for MTSET, MTSEA, and MTSES, respectively (Stauffer & Karlin, 1994), we used equireactive concentrations of 1 mM MTSET (A), 2.5 mM MTSEA (Figure 1A), and 10 mM MTSES (B). The means and SEM are shown. The number of independent experiments for each mutant is shown next to the bars. Solid bars indicate mutants for which inhibition was significantly different ($p < 0.05$) than that for C118S by one-way ANOVA. * represents no detectable binding.

binding of [^{3}H]-*N*-methylspiperone is irreversibly inhibited. Thus, we infer that 12 of the 25 residues tested are on the water-accessible surface of the D2 receptor. These residues are Leu407$^{(7.34)}$, Tyr408$^{(7.35)}$, Ser409$^{(7.36)}$, Ala410$^{(7.37)}$, Phe411$^{(7.38)}$, Thr412$^{(7.39)}$, Trp413$^{(7.40)}$, Tyr416$^{(7.43)}$, Asn418$^{(7.45)}$, Asn422$^{(7.49)}$, Pro423$^{(7.50)}$, and Tyr426$^{(7.53)}$ (Figure 1). The reactivity of Gly415$^{(7.42)}$ could not be assessed because the mutant G415C did not bind [^{3}H]-*N*-methylspiperone.[4]

The residues that form the surface of the binding-site crevice are a subset of the water-accessible residues. We infer that water-accessible residues are in the binding-site crevice if the reaction of the MTS reagents is retarded by competitive antagonists or agonists. The competitive antagonist sulpiride protected all of the residues except S409C. We were unable to test for sulpiride protection with the mutants Y408C and A410C because the extent of inhibition, although statistically significant, was too small.

The extent of protection by sulpiride varied considerably among the mutants (Figure 2). Protection of a substituted cysteine is most simply explained by its proximity to the sulpiride and [^{3}H]-*N*-methylspiperone binding site. Nevertheless, not every one of these residues needs to contact sulpiride. Sulpiride could protect residues deeper in the crevice by binding above them and blocking the passage of MTSEA from the extracellular medium toward the cytoplasmic end of the crevice. We also cannot rule out indirect effects through propagated structural changes for either the inhibition by the MTS reagents or the protection by sulpiride. Whatever the mechanism of irreversible inhibition by the

[4] The mutant G415C either does not reach the surface of the cell or does not bind [^{3}H]-*N*-methylspiperone. An aberrant disulfide bond between the new Cys in G415C and Cys385$^{(6.47)}$ in M6 could lead to either effect. This, however, is unlikely since, although C385S bound [^{3}H]-*N*-methylspiperone normally, the double mutant C385S and G415C did not bind at all (data not shown).

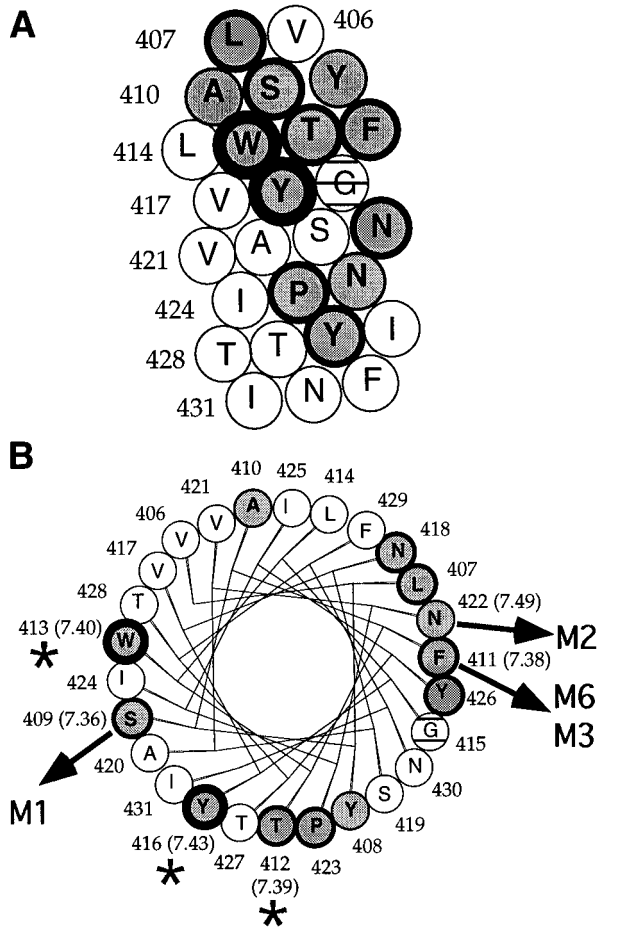

FIGURE 4: Helical net (A) and helical wheel (B) representations of the residues in and flanking the M7 segment of the dopamine D2 receptor, summarizing the effects of MTSEA on [^{3}H]-*N*-methylspiperone binding. Reactive residues are shaded, and the thickness of the circle indicates the range of the second-order rate constants in M^{-1} s^{-1} for reaction with MTSEA (see Table 3). Open circles indicate that MTSEA had no effect on binding. The hatched circle indicates no binding after cysteine substitution. In part B, residues, for which there is evidence in homologous receptors that they face the binding-site crevice, are indicated by *. The binding specificity of wild-type α2-adrenergic receptor can be converted to that of a β2-adrenergic receptor by substituting Asn for Phe412$^{(7.39)}$ (Suryanarayana et al., 1991); in β-adrenergic receptor, Trp330$^{(7.40)}$ is affinity labeled by two antagonist derivatives, and this labeling is blocked by specific β-adrenergic ligands (Wong et al., 1988). In rhodopsin, Lys296$^{(7.43)}$ is covalently attached to retinal (Oprian, 1992). Residues which are likely to face other membrane-spanning segments are indicated by an arrow pointing toward the membrane-spanning segments with which they likely interact. These annotations identify Asn422$^{(7.49)}$ which interacts with a residue in M2 (Sealfon et al., 1995; Zhou et al., 1994), Phe411$^{(7.38)}$ which interacts with residues in M3 and/or M6 (Mizobe et al., 1996), and Ser409$^{(7.36)}$ which interacts with a residue in M1 (Liu et al., 1995). If the arrangement of the membrane-spanning segments is as observed in the projection structure of rhodopsin [see Figure 6C and Schertler and Hargrave (1995)], then in the ideal α-helix shown, Asn422$^{(7.49)}$ could not interact with a residue in M2.

MTS reagents, the effect itself, however, is evidence that the reaction had occurred.

Secondary Structure of M7. On the basis of the structures of bacteriorhodopsin (Henderson et al., 1990) and rhodopsin (Schertler et al., 1993), the membrane-spanning segments of G-protein-coupled receptors have been modeled as α-helices (Baldwin, 1993). Others, however, based on NMR studies in the neurokinin I receptor (Berlose et al., 1994) and photolabeling studies in rhodopsin (Donnelly et al., 1989, Findlay & Pappin, 1986), have inferred deviations from regular α-helical structure in M7. We have found that the pattern of the residues which are accessible to the MTS reagents is not consistent with M7 being an ideal α-helix (Figure 4, Figure 6A). The irregular pattern of accessibility of substituted cysteines in M7, however, could be consistent with an α-helix with a proline kink (Pro kink) (Barlow & Thornton, 1988) at the strictly conserved Pro423$^{(7.50)}$.

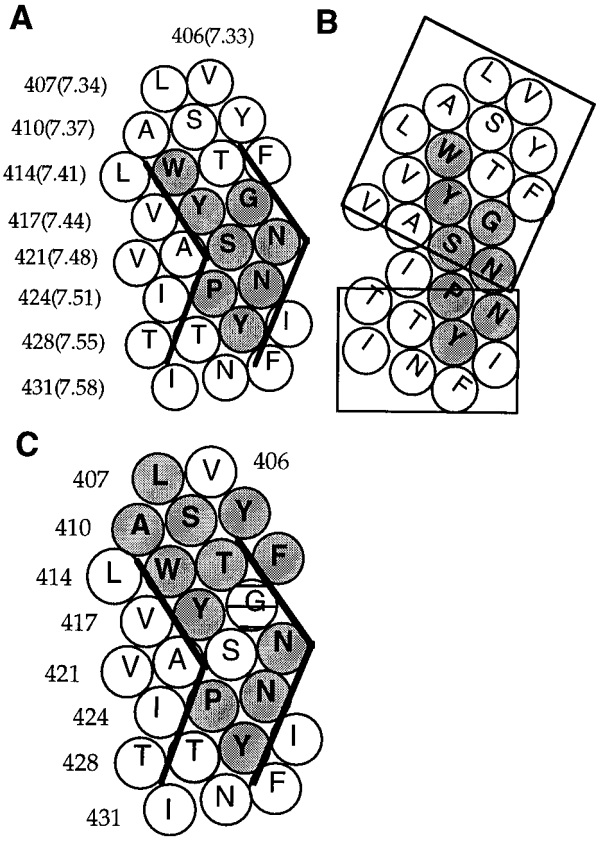

FIGURE 5: Helical net representation of highly conserved residues and residues accessible to MTSEA in M7. In parts A and B, the residues in M7 of the D2 receptor that are highly conserved in neurotransmitter−G-protein-coupled receptors are shaded. In part A, bold lines illustrate an apparent kink in the membrane-spanning segment, and in B, the segment is bent and twisted to illustrate how the conserved residues may lie on a single face of a kinked α-helix. In part C, the residues accessible to MTSEA are shaded and superimposed on the apparent kink from part A.

M7 had been modeled as a kinked α-helix on the basis of an analysis of the conservation of residues in neurotransmitter receptors (Ballesteros & Weinstein, 1995). Highly conserved residues were considered to play a critical structural role and to be involved in protein−protein interactions with other membrane-spanning segments (Ballesteros & Weinstein, 1995). This hypothesis is supported by an analysis of the known structure of the photosynthetic reaction center where highly conserved residues face the interior of the bundle (Rees et al., 1989). With a kink between Ser419$^{(7.46)}$ and Pro423$^{(7.50)}$, the highly conserved residues in the neurotransmitter receptors are aligned on a single face of an α-helix (Figure 5A,B). When such a kink is superimposed on the experimentally observed pattern of accessibility to MTSEA (Figure 5C), all accessible residues except the first helical turn (discussed below) are predicted to face toward the binding-site crevice or other membrane-spanning segments.

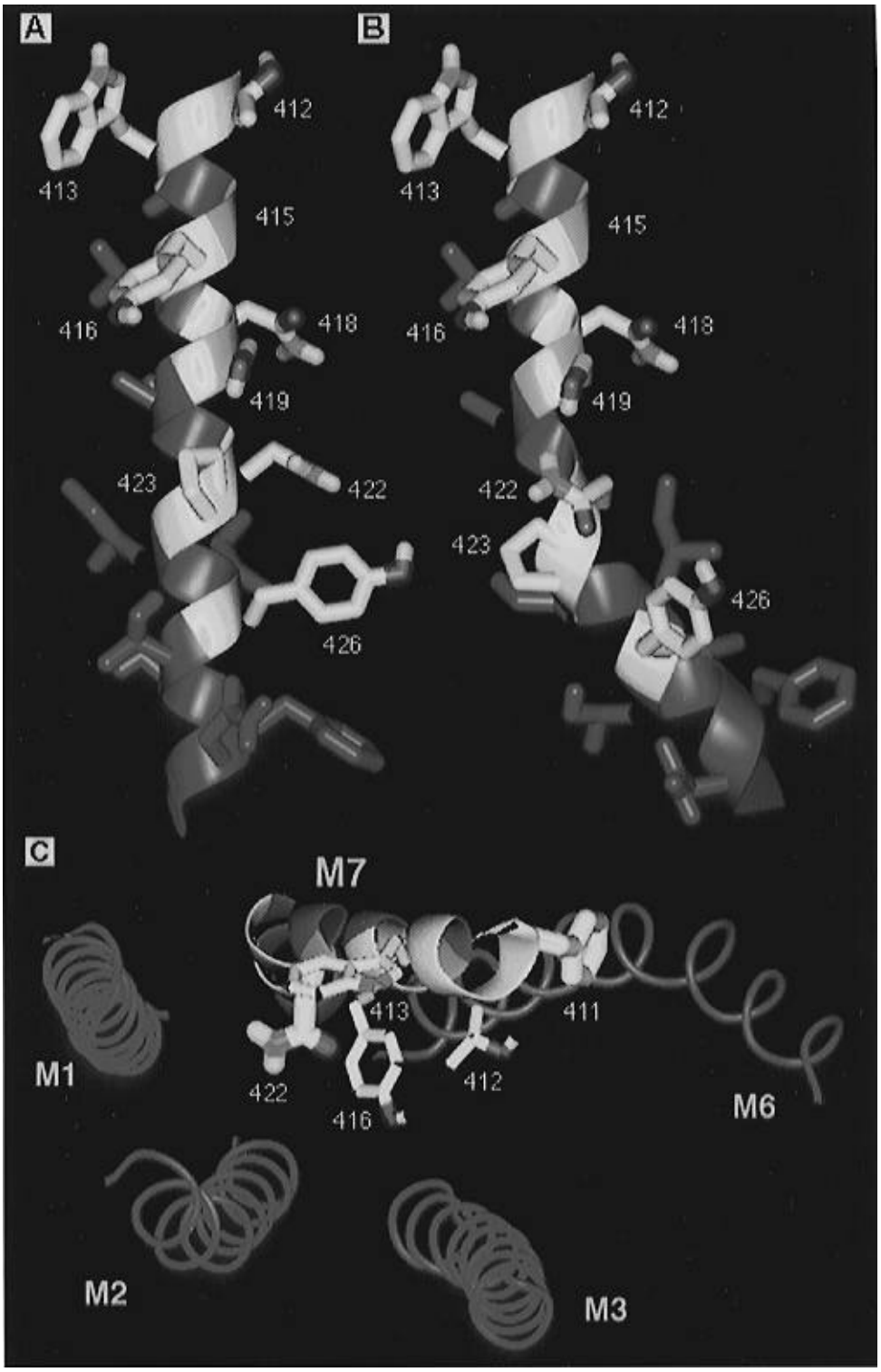

FIGURE 6: Molecular models of M7. The residues from Thr412$^{(7.39)}$ to Ile431$^{(7.58)}$ are shown (A) in an ideal α-helix and (B and C) in a kinked α-helix. The residues accessible to MTSEA are shown in yellow; Gly415$^{(7.42)}$ and Ser419$^{(7.46)}$ are shown in an olive color to emphasize their location on a continuous surface patch of accessible residues (see text); all other residues are shown in green and were not accessible to MTSEA. Note that in part A the accessible residues do not lie in one face. In parts B and C, all accessible residues now lie in a common face of the kinked α-helix. In part C, because of the twisting induced by the Pro kink, Asn422$^{(7.49)}$ is now oriented toward M2 and Phe411$^{(7.38)}$ is oriented towards M6 and M3, in agreement with experimental data (see the legend to Figure 4). Note that Thr412$^{(7.39)}$, Trp413$^{(7.40)}$, and Tyr416$^{(7.43)}$ all face the binding-site crevice.

Membrane-spanning segment interactions identified from experiments with double-revertant mutants are also not compatible with M7 being an ideal α-helix (Figure 4B and legend). In the context of a complete three-dimensional model of the receptor, the Pro kink in M7 as shown in Figure 6B,C incorporates both the bend illustrated in the helical net representation (Figure 5) and a twisting of the exposed faces of the helical segments before and after the Pro kink (Ballesteros & Weinstein, 1992; Sankararamakrishnan & Vishveshwara, 1992). The reorientation produced by the kink positions Asn422$^{(7.49)}$ toward M2, on a different face than Phe411$^{(7.38)}$ (Figure 6, legend to Figure 4). The modeled kink, while stronger than typically found, is within the observed range of kinks in known structures (Sankarara-

makrishnan & Vishveshwara, 1992). Interestingly, highly conserved Pro residues are found in M2, M5, M6, and M7 of GPCRs and may play a crucial structural and functional role (Ballesteros & Weinstein, 1992; Sansom, 1992; Williams & Deber, 1991; Woolfson et al., 1991). A possible mechanism of receptor activation utilizing Pro kink flexibility has been demonstrated (Luo et al., 1994; Zhang & Weinstein, 1993).

The modeled kink is also consistent with the pattern of accessibility to MTSEA seen in the current study (Figure 6B,C). Thr412$^{(7.39)}$, Trp413$^{(7.40)}$, Tyr416$^{(7.43)}$, Asn418$^{(7.45)}$, Asn422$^{(7.49)}$, Pro423$^{(7.50)}$, and Tyr426$^{(7.53)}$ all lie on a continuous surface patch based on such a model, and cysteines substituted for all of these residues react with MTSEA. In addition, the highly conserved Gly415$^{(7.42)}$ is predicted to be accessible, and while we could not assess this due to the fact that we obtained no binding to G415C, the pattern of accessibility surrounding Gly415$^{(7.42)}$ is consistent with its accessibility as well.

According to the model, Ser419$^{(7.46)}$ is located within a continuous surface patch on M7 that is accessible to MTSEA (Figure 6B,C). However, MTSEA had no significant effect on antagonist binding to S419C. There are several possible explanations for this discrepancy. First, if the structure of the mutant receptor deviates significantly from the native structure, the resulting accessibility of the new Cys in S419C may differ from that of Ser419$^{(7.46)}$. This Ser is highly conserved among GPCRs and is likely involved in a hydrogen-bonding network that modulates the Pro kink of M7.[5] However, while the affinity of S419C for sulpiride is decreased 8-fold, the normal binding of *N*-methylspiperone to S419C suggests the absence of a major structural perturbation. A second possibility is that side chain interaction within M7, or the packing of this region against other membrane-spanning segments, may sterically hinder access to the new Cys or change the ionization state of the new Cys, making it less reactive. A third possibility is that the actual structure of this "hinge" region in the receptor differs from the model used here.

Extracellular End of M7. At the extracellular end of M7, we observed that a continuous stretch of seven residues, from Leu407$^{(7.34)}$ to Trp413$^{(7.40)}$, was accessible to the MTS reagents. This pattern of accessibility is inconsistent with α-helical periodicity (Figure 4A). There are two plausible explanations for the observed pattern. First, the membrane-spanning segment may end at Phe411$^{(7.38)}$ or Thr412$^{(7.39)}$, making the residues from Val406$^{(7.33)}$ to Ala410$^{(7.37)}$ accessible in the M6−M7 loop. The rates of reaction of the cysteines substituted for these residues are consistent with an "every other" pattern of accessibility; i.e. Leu407$^{(7.34)}$, Ser409$^{(7.36)}$, and Phe411$^{(7.38)}$ are considerably more reactive than are the intervening residues (Figures 1 and 3A). This pattern suggests the presence of a β-strand in this region; cysteines substituted for residues which face away from the binding-site crevice, i.e. Val406$^{(7.33)}$, Tyr408$^{(7.35)}$, and Ala410$^{(7.37)}$, would have less of an effect on binding, even if they react with MTSEA. An alternative explanation is that this region may be α-helical and yet maintain the reactivity of consecutive residues toward MTSEA. The orientation of the $C_\alpha-C_\beta$ bond toward the N-terminal end of an α-helix may allow the side chains of all cysteines substituted for the residues in the first turn of an α-helix in M7 to protrude into the extracellular environment where they could react with MTSEA. Such an orientation-based reactivity is consistent with our finding that S409C, which would be on the opposite side of the α-helix, was not protected by the presence of sulpiride in the binding site.

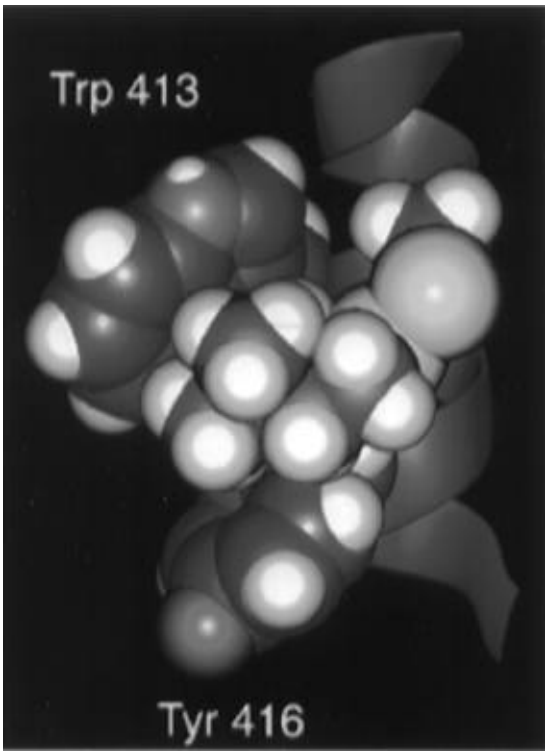

FIGURE 7: Molecular model showing the quaternary ammonium (in purple) of MTSET after reaction with T412C in van der Waals contact with the aromatic side chains of Trp413$^{(7.40)}$ and Tyr416$^{(7.43)}$.

Comparison of Reactions with MTSEA and MTSET. When adjusted for the rate constants for their reactions with simple thiols in solution (Stauffer & Karlin, 1994), the reaction of MTSEA with cysteines in the binding-site crevice is accelerated approximately 10-fold relative to that of MTSET (Figures 1 and 3A). MTSEA, like dopamine, contains an ethylammonium group, and it could be the affinity of this group for the dopamine-binding site that accelerates the reaction of MTSEA. This pattern is broken, however, by T412C, which is nearly equireactive with MTSEA and MTSET. Thus, at this position, the reaction of MTSET is accelerated approximately 10-fold relative to that of MTSEA. This specific increase may be the result of an interaction of the aromatic side chains of Trp413$^{(7.40)}$ and Tyr416$^{(7.43)}$ with the hydrophobic quaternary ammonium group of MTSET which stabilizes the product of the reaction with MTSET at T412C. The feasibility of this cation−π interaction (Dougherty, 1996) is illustrated in the model shown in Figure 7, where the $SCH_2CH_2N(CH_3)_3^+$ moiety of MTSET is covalently attached to T412C and the quaternary ammonium is shown to be positioned perfectly for intercalation between the aromatic side chains. This local interaction (Figure 7) is consistent both with the observed increase in reactivity and with the α-helical nature of this part of the structure.

SCAM and Tertiary Structure. It is interesting that MTSEA reacted with Cys substituted for residues proposed

[5] Note that Ser419$^{(7.46)}$ is $i - 4$ residues from Pro423$^{(7.50)}$.

to be involved in interactions among membrane-spanning segments. Specifically, the residues at 7.36, 7.38, and 7.49 have been proposed to have interactions with residues in M1, M3 and/or M6, and M2, respectively (see the legend to Figure 4) (Liu et al., 1995; Mizobe et al., 1996; Sealfon et al., 1995; Zhou et al., 1994). It is possible that substitution of Cys at these positions subtly alters the local interaction and makes the engineered Cys more accessible than is the wild-type residue, but the minimal effects of mutation to Cys on the binding of both *N*-methylspiperone and sulpiride argue against any significant perturbation in the structure of these Cys-substitution mutants. The present results may indicate that the dynamic structure of the receptor allows the access of water and MTSEA, at an appreciable rate, to residues involved in interactions among membrane-spanning segments.

ACKNOWLEDGMENT

We thank Dr. Olivier Civelli for the human D2 receptor cDNA, Dr. Jeremy Nathans for pRSVTag, Thomas Livelli for the HEK 293 cells and for valuable advice, Alexander Fariborzian for synthesizing the MTS reagents, and Dr. Myles Akabas, Dr. Arthur Karlin, and Merrill Martin for comments on the manuscript.

REFERENCES

Akabas, M. H., Stauffer, D. A., Xu, M., & Karlin, A. (1992) *Science 258*, 307−10.

Akabas, M. H., Kaufmann, C., Archdeacon, P., & Karlin, A. (1994) *Neuron 13*, 919−27.

Baldwin, J. M. (1993) *EMBO J. 12*, 1693−703.

Ballesteros, J. A., & Weinstein, H. (1992) *Biophys. J. 62*, 107−9.

Ballesteros, J. A., & Weinstein, H. (1995) *Methods Neurosci. 25*, 366−428.

Barak, L. S., Menard, L., Ferguson, S. S., Colapietro, A. M., & Caron, M. G. (1995) *Biochemistry 34*, 15407−14.

Barlow, D. J., & Thornton, J. M. (1988) *J. Mol. Biol. 201*, 601−19.

Berlose, J. P., Convert, O., Brunissen, A., Chassaing, G., & Lavielle, S. (1994) *Eur. J. Biochem. 225*, 827−43.

Civelli, O., Bunzow, J. R., Grandy, D. K., Zhou, Q. Y., & Van Tol, H. H. (1991) *Eur. J. Pharmacol. 207*, 277−86.

Donnelly, D., Johnson, M. S., Blundell, T. L., & Saunders, J. (1989) *FEBS Lett. 251*, 109−16.

Dougherty, D. A. (1996) *Science 271*, 163−8.

Findlay, J. B., & Pappin, D. J. (1986) *Biochem. J. 238*, 625−42.

Goldstein, A., & Barrett, R. W. (1987) *Mol. Pharmacol. 31*, 603−9.

Henderson, R., Baldwin, J. M., Ceska, T. A., Zemlin, F., Beckmann, E., & Downing, K. H. (1990) *J. Mol. Biol. 213*, 899−929.

Javitch, J. A., Li, X., Kaback, J., & Karlin, A. (1994) *Proc. Natl. Acad. Sci. U.S.A. 91*, 10355−9.

Javitch, J. A., Fu, D., Chen, J., & Karlin, A. (1995a) *Neuron 14*, 825−31.

Javitch, J. A., Fu, D., & Chen, J. (1995b) *Biochemistry 34*, 16433−9.

Javitch, J. A., Fu, D., & Chen, J. (1996) *Mol. Pharmacol. 49*, 692−8.

Kozell, L. B., Machida, C. A., Neve, R. L., & Neve, K. A. (1994) *J. Biol. Chem. 269*, 30299−306.

Liu, J., Schoneberg, T., van Rhee, M., & Wess, J. (1995) *J. Biol. Chem. 270*, 19532−9.

Luo, X., Zhang, D., & Weinstein, H. (1994) *Protein Eng. 7*, 1441−8.

MacKenzie, R. G., Steffey, M. E., Manelli, A. M., Pollock, N. J., & Frail, D. E. (1993) *FEBS Lett. 323*, 59−62.

Mizobe, T., Maze, M., Lam, V., Suryanarayana, S., & Kobilka, B. K. (1996) *J. Biol. Chem. 271*, 2387−9.

Oprian, D. D. (1992) *J. Bioenerg. Biomembr. 24*, 211−7.

Rees, D. C., Komiya, H., Yeates, T. O., Allen, J. P., & Feher, G. (1989) *Annu. Rev. Biochem. 58*, 607−33.

Roberts, D. D., Lewis, S. D., Ballou, D. P., Olson, S. T., & Shafer, J. A. (1986) *Biochemistry 25*, 5595−601.

Sankararamakrishnan, R., & Vishveshwara, S. (1992) *Int. J. Pept. Protein Res. 39*, 356−63.

Sansom, M. S. (1992) *Protein Eng. 5*, 53−60.

Schertler, G. F. X., & Hargrave, P. A. (1995) *Proc. Natl. Acad. Sci. U.S.A. 92*, 11578−82.

Schertler, G. F., Villa, C., & Henderson, R. (1993) *Nature 362*, 770−2.

Sealfon, S. C., Chi, L., Ebersole, B. J., Rodic, V., Zhang, D., Ballesteros, J. A., & Weinstein, H. (1995) *J. Biol. Chem. 270*, 16683−8.

Stauffer, D. A., & Karlin, A. (1994) *Biochemistry 33*, 6840−9.

Strader, C. D., Candelore, M. R., Hill, W. S., Sigal, I. S., & Dixon, R. A. (1989) *J. Biol. Chem. 264*, 13572−8.

Strader, C. D., Fong, T. M., Tota, M. R., Underwood, D., & Dixon, R. A. (1994) *Annu. Rev. Biochem. 63*, 101−32.

Suryanarayana, S., Daunt, D. A., Von, Z. M., & Kobilka, B. K. (1991) *J. Biol. Chem. 266*, 15488−92.

Teeter, M. M., & DuRand, C. J. (1996) *Drug Dev. Res.* (in press).

van Rhee, A. M., & Jacobson, K. A. (1996) *Drug Dev. Res. 37*, 1−38.

Williams, K. A., & Deber, C. M. (1991) *Biochemistry 30*, 8919−23.

Wong, S. K., Slaughter, C., Ruoho, A. E., & Ross, E. M. (1988) *J. Biol. Chem. 263*, 7925−8.

Woolfson, D. N., Mortishire, S. R. J., & Williams, D. H. (1991) *Biochem. Biophys. Res. Commun. 175*, 733−7.

Zhang, D., & Weinstein, H. (1993) *J. Med. Chem. 36*, 934−8.

Zhou, W., Flanagan, C., Ballesteros, J. A., Konvicka, K., Davidson, J. S., Weinstein, H., Millar, R. P., & Sealfon, S. C. (1994) *Mol. Pharmacol. 45*, 165−70.

BI960928X